Wave Motion 51 (2014) 1170–1178

Contents lists available at ScienceDirect

Wave Motion

journal homepage: www.elsevier.com/locate/wavemoti

# A facile method to realize perfectly matched layers for elastic waves

Zheng Chang [a,b], Dengke Guo [a], Xi-Qiao Feng [b], Gengkai Hu [a,*]

[a] Key Laboratory of Dynamics and Control of Flight Vehicle, Ministry of Education, School of Aerospace Engineering, Beijing Institute of Technology, Beijing 100081, China

[b] CNMM & AML, Department of Engineering Mechanics, Tsinghua University, Beijing 100084, China

## HIGHLIGHTS

- The design method of PMLs is proposed based on transformation elastodynamics.
- The PML can be easily realized by functionally graded viscoelastic materials.
- Numerical simulations are performed to validate the performance of the PMLs.

## ARTICLE INFO

*Article history:*
Received 8 January 2014
Received in revised form 26 June 2014
Accepted 4 July 2014
Available online 18 July 2014

*Keywords:*
Perfectly matched layers
Elastodynamics
Conformal transformation
Elastic waves

## ABSTRACT

In perfectly matched layer (PML) technique, an artificial layer is introduced in the simulation of wave propagation as a boundary condition which absorbs all incident waves without any reflection. Such a layer is generally thought to be unrealizable due to its complicated material formulation. In this paper, on the basis of transformation elastodynamics and complex coordinate transformation, a novel method is proposed to design PMLs for elastic waves. By applying the conformal transformation technique, the proposed PML is formulated in terms of conventional constitutive parameters and then can be easily realized by functionally graded viscoelastic materials. We perform numerical simulations to validate the material realization and performance of this PML.



## 1. Introduction

In 1994, Berenger [1] proposed a perfectly matched layer (PML) technique to improve the efficiency of wave propagation simulations. A PML is an artificial layer introduced as boundary conditions in calculation model, which absorbs all incident waves without any reflection. The key strategy in this technique is to perform a coordinate transformation which maps the real harmonic wave $e^{i\mathbf{k}\cdot\mathbf{x}}$ in the real space $\mathbf{x}$ into the following form in a complex space $\hat{\mathbf{x}} = \mathbf{x}' + i\mathbf{x}''$:

$$e^{i\mathbf{k}\cdot\hat{\mathbf{x}}} = e^{-\mathbf{k}\cdot\mathbf{x}''} e^{i\mathbf{k}\cdot\mathbf{x}'}, \tag{1}$$

where $\mathbf{k}$ is the wavevector. Thus the coordinate transformation makes the wave attenuate in the exponential manner $e^{-\mathbf{k}\cdot\mathbf{x}''}$. In the early understanding, the PMLs were thought to be "nonphysical" and "purely mathematical". Later, an alternative formulation of PMLs in electrodynamics was reported [2,3], known as "Maxwellian PMLs", in which the coordinate deformation

* Corresponding author. Tel.: +86 10 68918363; fax: +86 10 68914538.
*E-mail address:* hugeng@bit.edu.cn (G. Hu).

http://dx.doi.org/10.1016/j.wavemoti.2014.07.003
0165-2125/

is described by complex material parameters. These works not only revealed the physical interpretation of PMLs but also showed the possibility of their realization in practical materials.

Coincidentally, the similar idea of equivalence between material distribution and space distortion has been employed in the transformation method (TM) [4,5], or more specifically, the transformation optics (TO) in the field of electrodynamics, to design novel wave functional devices, such as "invisibility cloak" [6]. Teixeira et al. [7] investigated the relation between the PML method and the TM method. They demonstrated that the complex transformation in the former method can be regarded as a generalization of the latter. It is also noticed that in the field of elastodynamics, there is a similar coincidence. The material formulation of elastodynamic PMLs [8] has the same form as that derived by transformation elastodynamics [9] with the stiffness tensor without minor symmetry. Recently, Chang et al. [10,11] designed a simplified form of elastodynamic PMLs with a symmetric elastic tensor on the basis of an approximate transformation elastodynamic method. This type of PMLs have been proved by a number of numerical examples to have good absorption property [10,11], but it remains unclear how they can be realized in practice. In addition, the TM has been demonstrated as a convenient tool to elucidate the physical insight of PMLs and to ease the design process of PMLs. For instance, Popa et al. [12] used this technique to design an electromagnetic PML of arbitrary shape in the context of transformation optics. In the present study, the TM will be used to design elastodynamic PMLs and to simplify the designed PMLs to a realizable level.

As PMLs are mathematically formulated in a complex space, their realization by real materials is a technologically important issue. In elastodynamics, a good absorption ability to incident wave is of great interest in both experimental and engineering applications. Especially, if there is no effective absorption mechanism, elastic waves could not be measured in steady state in elastodynamic experiments. Even in transient measurements, the sample has to be very large in order to avoid the interference of reflected waves from boundaries. For a long time, the PML technique has not been realized in practice but only used in numerical simulations. The main obstacle to realize the PML technique is that the mathematically derived PMLs require asymmetric elastic tensors [8], which do not exist in nature. This difficulty will be overcome in the present paper by applying conformal transformation technique.

In this study, a design method of an elastodynamic PML is proposed on the basis of transformation elastodynamics. We will show that an elastodynamic PML can be formulated in terms of conventional material parameters and can be fabricated with conventional viscoelastic materials. The paper is organized as follows. In Section 2, an elastodynamic PML is proposed on the basis of transformation elastodynamics and validated via a number of numerical simulations. In Section 3, the formulation of the proposed PML is further simplified to make them physically realizable. Especially, a simple prototype of PMLs is given. Finally, the main results are summarized in Section 4.

## 2. Elastodynamic PML

In this section, we first derive the formulation of elastodynamic PMLs by using the TM. The governing equation of elastic waves, Navier's equation, is written as [10]

$$\nabla \cdot \mathbf{C} : \nabla \mathbf{u} = -\omega^2 \boldsymbol{\rho} \cdot \mathbf{u}, \tag{2}$$

where $\mathbf{C}$ is the fourth-order elastic tensor, $\mathbf{u}$ is the wave displacement vector, $\boldsymbol{\rho}$ is the anisotropic mass density tensor, and $\omega$ is the angular frequency. As the core of transformation elastodynamics, the form invariance of Eq. (2) under coordinate transformation has been investigated by various methods [9–11,13,14]. Milton et al. [13] first raised the problem and showed by so-called "change of variable" approach that Navier's equation in (2) will not preserve its original form but will be transformed into Willis' equation under the prescribed transformation relation of displacement

$$\bar{\mathbf{u}} = \mathbf{A}^{-T}\mathbf{u}, \tag{3}$$

where $A_{Nn} = \partial x_N / \partial X_n$ is the Jacobian matrix of space (or coordinate) transformation. This implies the transformation method can only be available under the condition that the transformed material obeys Willis equation. Later, Brun et al. [9] demonstrated a precise control of elastic wave by using transformation method with the following transformation relation of displacement vector

$$\bar{\mathbf{u}} = \mathbf{I}\mathbf{u}, \tag{4}$$

where $I_{li} = \delta_{li}$ is the second-order unit tensor. In this method, the transformed material is of Navier's form, but the asymmetric elastic tensor is needed to guarantee the form invariance. Furthermore, Norris and Shuvalov [14] developed a general elastic cloaking theory in which a "gauge" matrix is applied such that both above two works are particular cases of the theory. On the other hand, Chang et al. [10] proposed an alternative method to obtain possible transformation relations which can keep the form of governing equations (e.g. Maxwell equations for electromagnetic waves and Helmholtz equation for acoustic waves) during coordinate transformation. They found for elastodynamics, the form invariance of Eq. (2) can be approximately preserved in case where the gradient of the elastic moduli of the transformed material is small or when wave frequency is high [11].

By introducing complex coordinate transformation, the above methods can all be applied to accomplish the design of PMLs. However, for the ease of numerical implementation and further simplification, only Navier's form of transformed material is considered in this work.

In the above specification, only two sets of transformation relations need to be considered. For example, one can use Brun's transformation relations [9] (or equivalently Norris and Shuvalov's with the "gauge" matrix equals to **I**, see Ref. [14]),

$$\begin{aligned}\bar{C}_{IJKL} &= J^{-1}A_{Ii}I_{Jj}A_{Kk}I_{Ll}C_{ijkl},\\ \bar{\rho} &= J^{-1}\rho,\end{aligned} \tag{5}$$

where $J = \det(A_{Nn})$ is the Jacobian. Using Eq. (5), the material parameters in the initial virtual space $C_{ijkl}$ and $\rho$ are transformed into $\bar{C}_{IJKL}$ and $\bar{\rho}$ in the physical space, respectively. Correspondingly, the wave displacement vector in the virtual space is mapped to in the physical space according to Eq. (4). The above relations constitute the basis of such wave control devices as "elastodynamic cloak" [9]. However, if one follows this path to design a PML for elastic waves, the transformed elastic tensor $\bar{C}_{IJKL}$ will lose its minor symmetry, making the material realization very difficult.

Another method [11] can also be used with the following material transformation relations:

$$\begin{aligned}\bar{C}_{IJKL} &= J^{-1}A_{Ii}A_{Jj}A_{Kk}A_{Ll}C_{ijkl},\\ \bar{\rho}_{IJ} &= J^{-1}A_{Ii}A_{Jj}\delta_{ij}\rho.\end{aligned} \tag{6}$$

Correspondingly, the wave displacement vector **u** in the virtual space will be approximately mapped into the physical space via the relation of Eq. (3). These relations are identical to Milton's Willis-form-relations [13] (or equivalently Norris and Shuvalov's with the "gauge" matrix equals to **A**, see Ref. [14]). A simplification is made by neglecting all the terms containing the partial derivative of **A** in the Willis' equation to approximately preserve the form of Eq. (2), this leads to Eq. (6). The accuracy of this approximate method was evaluated and discussed in [11,15]. The imperfection of this method can also be observed in later PML design processes. It is noted that when the space mapping is conformal, the designed transformation devices will perform well at any material gradient or wave frequency [16,17]. In addition, the relation in Eq. (6) can guarantee the symmetry of the elastic tensor, a distinct advantage for PML realization over that in Eq. (5). However, it is still difficult, if not impossible, to achieve the anisotropic dynamic mass density assumed in Eq. (6).

In 2009, Hu et al. [18] proposed a representation method of transformation relation, in which the coordinate transformation is described as space deformation. By applying polar decomposition, the Jacobian matrix can be expressed as $\mathbf{A} = \mathbf{V}\cdot\mathbf{R}$. Here **R** is an orthogonal tensor describing the rigid rotation of the local infinitesimal element, and **V** is a symmetric tensor with eigenvalues $\lambda_I$ ($I = 1, \ldots, N$) denoting the stretch of a local infinitesimal element, where $N$ is the dimension of the problem under study and $\lambda_I$ is the linear principal stretch in the $I$-direction. Thus in the local principal coordinates $\hat{e}_I$, **V** can be expressed as a diagonal form $\mathbf{V} = \sum_1^N \lambda_I \hat{e}_I\hat{e}_I$. As the rigid rotation does not change the property of infinitesimal elements during the "space deformation", we rewrite the transformation relations in Eqs. (5) and (6) into simpler forms in terms of local principal coordinates $\hat{e}_I$. Then Eq. (5) becomes a very simple form:

$$\begin{aligned}\bar{C}_{IJKL} &= J^{-1}\lambda_I\lambda_K C_{ijkl},\\ \bar{\rho} &= J^{-1}\rho,\end{aligned} \tag{7}$$

where a capital index in the subscript takes the same value as its corresponding lower index, and $J = \sum_{I=1}^N \lambda_I$. As aforementioned, **V** is a diagonal matrix in the local principal coordinates, Einstein summation convention is not adopted for a capital index and its lower counterpart. Similarly, Eq. (6) is rewritten as [11]

$$\begin{aligned}\bar{C}_{IJKL} &= J^{-1}\lambda_I\lambda_J\lambda_K\lambda_L C_{ijkl},\\ \bar{\rho}_{IJ} &= J^{-1}\lambda_I\lambda_J\delta_{ij}\rho.\end{aligned} \tag{8}$$

This representation has the advantage that the interference of rotation terms has been ruled out, and thus the physical insight during the "space transformation" can be revealed clearly. Particularly, in the case when the local principal coordinate is identical with the original coordinate (no rotation during the global transformation), Eqs. (7) and (8) can be seen as the global transformation relations with $\lambda_I$ being the stretch function along $I$ direction. In this sense, Eqs. (7) and (8) imply that we can design transformation devices using $\lambda_I$ without considering the specific form of space mapping. This will greatly simplify the design of PMLs, as we show below.

Now we discuss the design of elastodynamic PMLs. As mentioned above, complex principal stretches are applied to introduce the attenuation of waves. To create a PML which can absorb the $x$-component of incident elastic waves in a two-dimensional (in-plane) problem, as shown in Fig. 1, the local principal directions at position $(x, y)$ should be identical with the directions of the unit vectors in the global Cartesian coordinate system. Then we choose the principal stretches as

$$\lambda_x = 1 + i\beta(x), \qquad \lambda_y = 1 \tag{9}$$

where $\beta(x)$ is a tunable function. One can choose the function $\beta(x)$ according to the absorption efficiency of the PML. Substituting Eq. (9) into Eqs. (7) and (8) renders two design methods of elastodynamic PMLs. It is emphasized that the two methods are different in their impedance match conditions for the following reason. In Eq. (7), $\beta(x)$ can be arbitrarily chosen, because the impedance matched condition on the wave incident boundary $\partial\Omega$ is an intrinsic feature in asymmetric TM [9]. In contrary, for the approximate method defined by Eq. (8), $\beta(x)$ should satisfy the $C_0$ continuity on $\partial\Omega$, i.e.,

$$\beta(x)|_{\partial\Omega} = 0, \tag{10}$$

such that the mapping has the $C_1$ continuity on the boundary. Only in this case, can the designed PML perfectly match the computational domain [11].

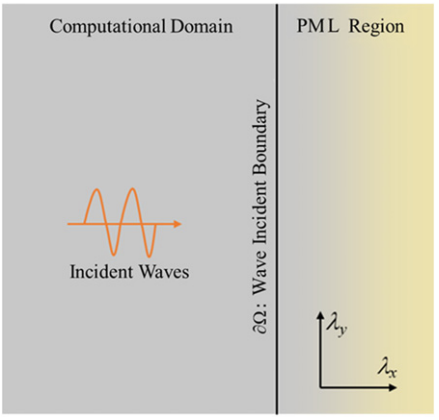


**Fig. 1.** Schematic diagram of a PML, where $\partial\Omega$ is the wave incidence boundary, $\lambda_x$ and $\lambda_y$ are the principal stretches in the PML during space transformation.

In what follows, we will discuss the numerical implementation of this type of elastodynamic PMLs and show the difference between the PMLs derived from Eqs. (7) and (8).

For illustration, we consider a 1 m × 1 m square computational domain centroid at (0, 0). Its boundary is surrounded by eight PML domains with width $l = 0.1$ m, numbered as I to VIII, respectively. A source of circular shape with the radius $w = 0.01$ m and the center at $(-0.3, 0.3)$ is set to emit *P*- or *S*-waves, as shown in Fig. 2. For the *normalized* material parameters of the computational free space, we set the Lame constants $La_1 = 2.3$ and $La_2 = 1$ and the mass density $\rho = 1$. According to Eq. (9), to ensure that the PMLs can absorb incident waves from any directions, the principal stretches in the eight PML domains should have the following form:

$$\begin{aligned}
&\lambda_x = 1 + i\beta(x - x_{wi}), \qquad \lambda_y = 1 \text{ (in domains I and II)};\\
&\lambda_x = 1, \qquad \lambda_y = 1 + i\beta(y - y_{wi}) \text{ (in domains III and IV)};\\
&\lambda_x = 1 + i\beta(x - x_{wi}), \qquad \lambda_y = 1 + i\beta(y - y_{wi}) \text{ (in domains V–VIII)},
\end{aligned} \tag{11}$$

where $x_{wi}$ and $y_{wi}$ are the $x$ and $y$ coordinates at the wave incident boundaries, respectively. For the example shown in Fig. 2, we have $x_{wi} = -0.5$ for domains I, V and VII, and $x_{wi} = 0.5$ for domains II, VI and VIII. Similarly, we have $y_{wi} = 0.5$ for domains III, V and VI, and $y_{wi} = -0.5$ for domains VI, VII and VIII.

For PMLs governed by Eq. (7), we can set $\beta(r - r_{wi})(r = x, y)$ in Eq. (11) as a constant, i.e.

$$\beta(r - r_{wi}) = 1. \tag{12}$$

With the material parameters of free space, together with principal stretches expressed by Eqs. (11) and (12), the material parameters of the PML domains can be derived from Eq. (7). It is interesting to find that in this case, all designed PMLs have homogeneous material parameters. We simulate the PMLs using the weak form PDE module of finite element software, COMSOL Multiphysics. The results show that the PMLs can perfectly absorb the incident *P*- and *S*-waves from any angle, as illustrated in Fig. 3(a) and (b), respectively, where the waves emitted from the source have the angular frequency of $\omega = 200$ Hz and amplitude $B = 100$ μm.

A similar manipulation can be made to the PMLs expressed by Eq. (8) except that more constraints should be considered in the selection of $\beta(r - r_{wi})$, where $r = x, y$. Considering the continuity condition in Eq. (10), we may choose

$$\beta(r - r_{wi}) = 10\,|r - r_{wi}|\,. \tag{13}$$

Correspondingly, with the material parameters of free space, together with principal stretches expressed by Eqs. (11) and (13), the material parameters of the PML domains can be derived from Eq. (8). The numerical simulations show the PMLs also exhibit good absorbing performance for both *P*- and *S*-waves, as shown in Fig. 3(c) and (d). However, since the TM applied here is an approximate one, some slight scattering can be observed near the boundaries of the computational domain (Fig. 3(c) and (d)). To clearly indicate this imperfection, the absolute values of total displacement $\left|\sqrt{u_x^2 + u_y^2}\right|$ on two auxiliary segments $L_1$ and $L_2$ (see Fig. 2) are illustrated in Fig. 5(a) and (b), respectively. It is shown in Fig. 5(a) that for both *P*- and *S*-waves, the total displacement quickly decays in PML domains derived from both asymmetric (labeled as Case 1 in Fig. 5) and symmetric (labeled as Case 2 in Fig. 5) transformation relations. However, for the case of the symmetric transformation relations (Case 2), wave pattern (scattering) can be found in free space domain, which displays the imperfection of the corresponding PML. This imperfection can be more clearly illustrated in Fig. 5(b), which shows that the scattered wave on $L_2$ is much larger for symmetric transformation relations (Case 2) than that of asymmetric transformation relations (Case 1), although it can hardly be noticed in Fig. 3. A simple method to further reduce the scattering resulted from symmetric

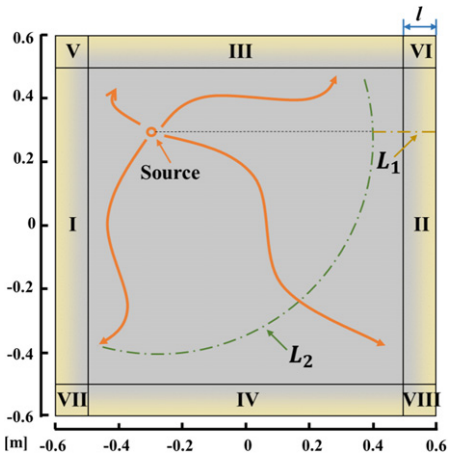


**Fig. 2.** Model of the PML numerical simulation. I–VIII denote the eight PML domains surrounding the computational domain, and the circular source in the free space emits $P$- or $S$-waves. $L_1$ and $L_2$ are two auxiliary segments to probe the total displacement, so as to illustrate the effectiveness of the PMLs.

transformation relations is to increase the PML thickness and, simultaneously, reduce the varying gradient of the principal stretches. For example, if we double the thickness of the PML by taking $l = 0.2$ m, the function $\beta(r - r_{wi})$ can be chosen as

$$\beta(r - r_{wi}) = 10\,|r - r_{wi}|^2\,. \tag{14}$$

In this case, no scattering is observed in the simulation results, as shown in Fig. 4(a) and (b) for $P$- and $S$-wave cases, respectively. The good performance of the proposed PMLs is also demonstrated in Fig. 5 (labeled Case 3). It is shown that the scattering of the modified symmetric PMLs is reduced to the same level as that of the asymmetric PMLs (Case 1).

## 3. Elastodynamic PMLs with realizable material parameters

Now we address the realization of the proposed PMLs. By substituting Eqs. (11) and (12) into (7), it is found that the formulation of the homogeneous PML contains both positive and negative imaginary parts in $\bar{C}_{IJKL}$. In contrast to the positive imaginary part, the negative imaginary part indicates a gain characteristic of the adopted material, which typically does not exist in conventional materials. Therefore, though the PML proposed in Section 2 is efficient in the numerical simulations of elastic waves, it is still hard to be realized in experiments or measurements. This issue will undoubtedly make the implementation of the PML in practical application difficult.

To solve this problem, the conformal transformation technique is utilized to simplify the material formulation of the proposed PMLs. As demonstrated in Ref. [5], a specific conformal transformation in TM can yield the isotropy of the transformed material parameters. Also importantly, one may choose different transformation relations for a conformal transformation [16]. We will utilize this feature to adjust the transformation relation such that the constitutive parameters of the PMLs can be realized in real materials. Furthermore, the conformal transformation is equivalent to Cauchy–Riemann condition. In terms of the above representation method suggested by Hu et al. [18], this condition can be simplified as

$$\lambda_x = \lambda_y = \lambda, \tag{15}$$

meaning that the infinitesimal element experiences the same stretch in all principal directions. It is interesting to see that with Eq. (15), the material transformation relations in Eqs. (7) and (8) are expressed in an identical form [16]:

$$\begin{aligned} \bar{C}_{IJKL} &= \lambda_{\mathrm{III}}^{-1} C_{ijkl}, \\ \bar{\rho} &= J^{-1}\lambda_{\mathrm{III}}^{-1}\rho, \end{aligned} \tag{16}$$

where $\lambda_{\mathrm{III}}$ is a tunable parameter. $\lambda_{\mathrm{III}} = 1$ and $\lambda_{\mathrm{III}} = \lambda^{-2}$ correspond to Eqs. (7) and (8), respectively. In two-dimensional problems, the tunable parameter $\lambda_{\mathrm{III}}$ can be seen as a virtual principal stretch in the out-of-plane direction. This parameter has been adopted in transformation acoustics [19] to eliminate the material singularity at the inner layer of acoustic cloaks.

In this study, we apply the similar idea to simplify the material parameters of the designed elastodynamic PMLs shown in Fig. 1. To introduce the attenuation of waves, we set

$$\lambda = 1 + i\beta(x). \tag{17}$$

Here, the function $\beta(x)$ should satisfy the following condition

$$\beta(x)|_{\partial\Omega} = 0, \tag{18}$$

such that the material parameters are continuous across the interface between the computational/experimental domain and the PMLs.

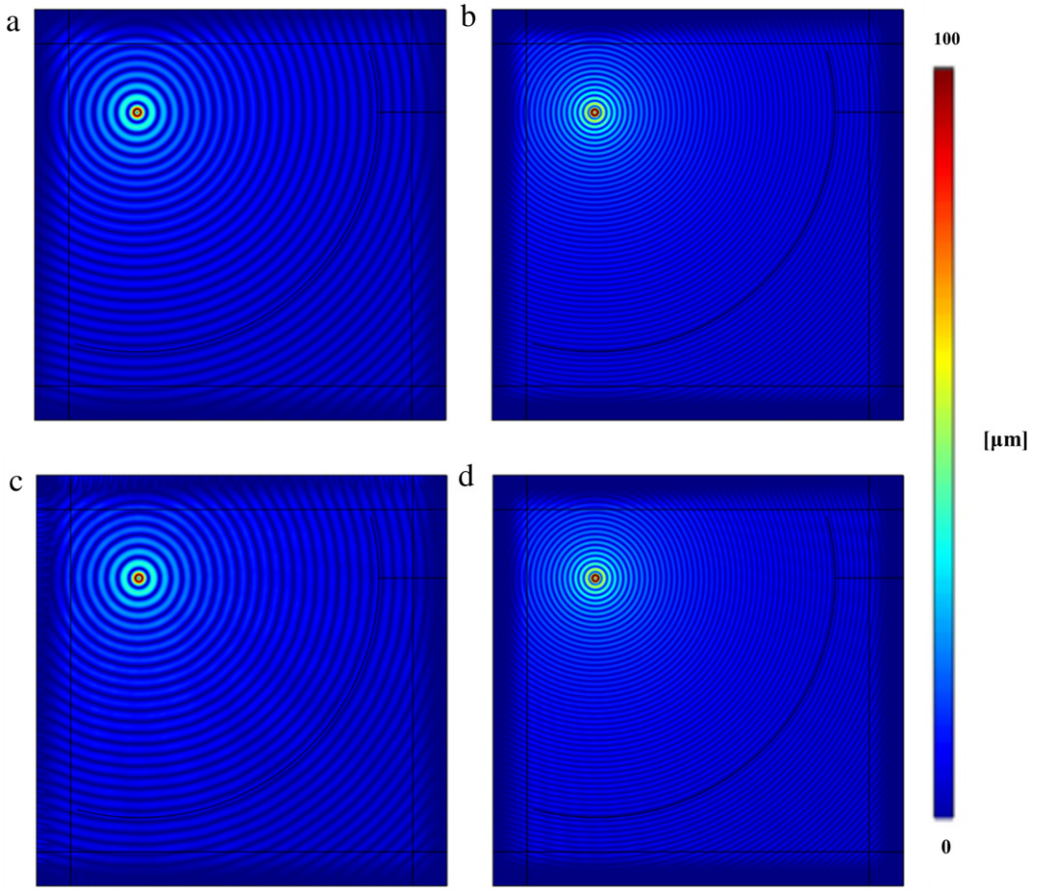


**Fig. 3.** Simulation results for the total wave displacement field $\sqrt{u_x^2 + u_y^2}$ in the computational domain and the PML domains for different cases: (a) PML designed with asymmetric TM, *P*-wave, (b) PML designed with asymmetric TM, *S*-wave, (c) PML designed with symmetric TM, *P*-wave, (d) PML designed with symmetric TM, *S*-wave.

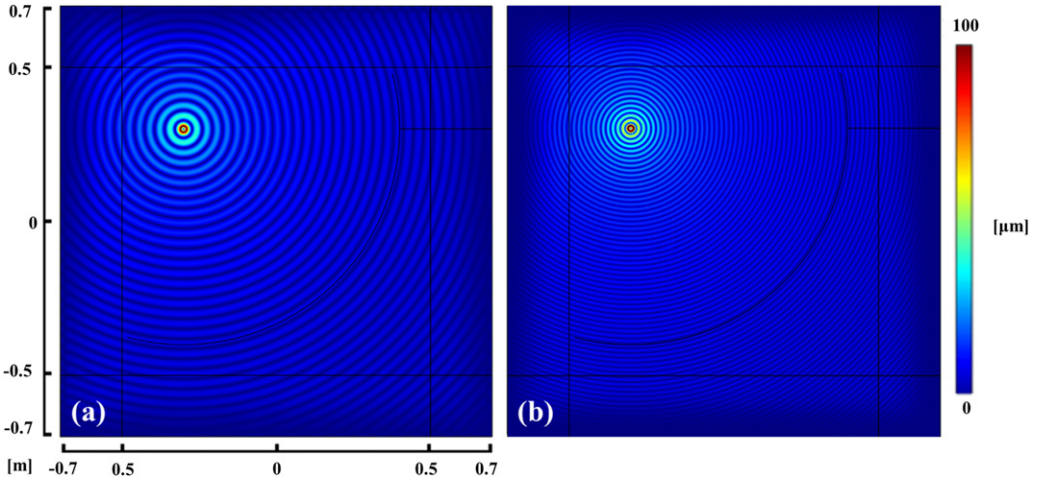


**Fig. 4.** Simulation results for the total wave displacement field $\sqrt{u_x^2 + u_y^2}$ in the computational domain and the PMLs designed with symmetric TM: (a) *P*-wave, (b) *S*-wave. Here, the width of the PML domains is doubled, while the imaginary part of the principal stretches is decreased of that in Fig. 3(c) and (d).

To further simplify the transformation relation, as aforementioned, one can choose $\lambda_{\underline{\underline{III}}} = 1$ or $\lambda^{-2}$ in Eq. (16), by which the attenuation characteristic will be ascribed to only a single material parameter, $\bar{\rho}$ or $\bar{C}$. First, we prefer the selection of

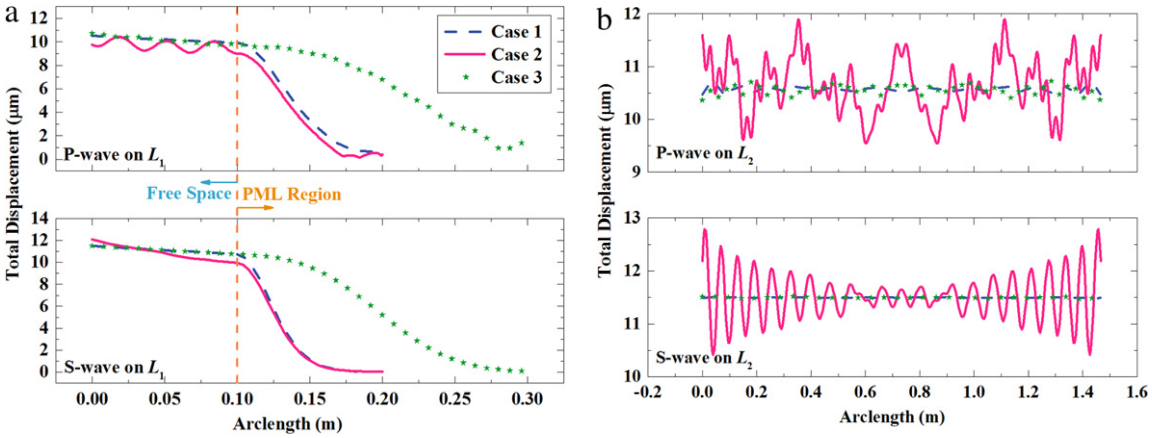


**Fig. 5.** Absolute values of total displacement $\left|\sqrt{u_x^2+u_y^2}\right|$ on auxiliary segments (a) $L_1$ and (b) $L_2$ for different cases. Case 1: PMLs designed with asymmetric transformation relations (corresponding to Fig. 3(a) and (b)). Case 2: PMLs designed with symmetric transformation relations (corresponding to Fig. 3(c) and (d)). Case 3: PMLs designed with symmetric transformation relations, but larger PML domains and smaller varying gradient of principal stretches than that of Case 2 (corresponding to Fig. 4(a) and (b)).

$\lambda_{\mathrm{III}} = \lambda^{-2}$, because following this selection, the obtained material parameters

$$\bar{E} = \left[1-\beta^2(x)\right]E + 2i\beta(x)E, \qquad \bar{\upsilon} = \upsilon, \qquad \bar{\rho} = \rho \tag{19}$$

have the same material formulation as that for isotropic viscoelastic materials, in which $E$ is the Young's modulus and $\upsilon$ the Poisson's ratio. On the other hand, if we choose $\lambda_{\mathrm{III}} = 1$, the dissipation term will be ascribed into the mass density, $\bar{\rho}$, which is not as easy as that in Eq. (19) in practical realization.

Eq. (19) provides a rather simple material formulation of a PML. However, its realization has two further difficulties. One is the simultaneous control of the four parameters of $real(\bar{E})$, $imag(\bar{E})$, $\bar{\upsilon}$ and $\bar{\rho}$, and the other is the production of a viscoelastic material with graded distribution $E$ but constant $\upsilon$ and $\rho$. We found these two difficulties can be easily overcome by considering the constraints of material parameters in the initial virtual space. In conventional TMs, the virtual space is usually assumed as a free space with isotropic and homogeneous material parameters. In fact, this assumption is unnecessary and can be eliminated because the transformation relation is applicable to an initial space with arbitrary distribution of material parameters [10]. In recognition of this important property of TM, therefore, the initial virtual space of the PML domain is here specified with material properties which smoothly vary along the $x$-direction, (i.e. substitute $E$, $\upsilon$ and $\rho$ in Eq. (19) with $E(x)$, $\upsilon(x)$ and $\rho(x)$) and are continuous with the computational/ experimental domain at the interface $\partial\Omega$ (e.g. $E(x)|_{\partial\Omega} = E$). In this case, if we define $\tilde{E}(x) = \left[1-\beta^2(x)\right]E(x)$, $\tilde{G}(x) = 2\beta(x)E(x)$, $\tilde{\upsilon}(x) = \upsilon(x)$ and $\tilde{\rho}(x) = \rho(x)$, respectively, the specific form of $\beta(x)$ becomes unimportant and the material parameters of the PML, Eq. (19), can be re-expressed as

$$\bar{E} = \tilde{E}(x) + i\tilde{G}(x), \qquad \bar{\upsilon} = \tilde{\upsilon}(x), \qquad \bar{\rho} = \tilde{\rho}(x), \tag{20}$$

which correspond to a functionally graded viscoelastic material.

The utilization of the functionally graded property in Eq. (20) makes the implementation of PMLs much easier. For example, the PML can be made by a viscoelastic material containing inclusions with a specific distribution in space. Its effective constitutive parameters can be predicted by such micromechanics methods as Mori–Tanaka method or the self-consistent method. In what follows, a simple prototype of such a PML will be given for illustration. For the matrix phase of the proposed PML and also for the material in the computational/experimental domain, we chose a structural steel, since steels are widely used in elastic wave experiments. Its mechanical parameters are taken as: mass density $\rho = 7850\ \mathrm{kg/m^3}$, Young's modulus $E = 200$ GPa, Poisson's ratio $\upsilon = 0.33$, and loss tangent $\delta = \arctan(G/E) \approx 0$ [20]. Silicone is used as the viscoelastic inclusion phase in the PML, which has $\rho = 2.3\ \mathrm{kg/m^3}$, $E = 0.05$ GPa, $\upsilon = 0.47$ and $\delta = 1.6$ [20]. The larger value of $\delta$ is beneficial to the design of a viscoelastic material with specific functionally graded properties. For example, consider a PML with the size 1 m $\times$ 0.2 m, as shown in Fig. 6(a). We discrete it into 20 layers with the same height (0.01 m) along the $y$-direction. Circular inclusions are added in the prototype. The radius of inclusions, $r_{\mathrm{inc}}$, linearly varies from 0.001 m to 0.0048 m along the $y$-direction. Along the $x$-direction, the inclusions are uniformly distributed with distance of 0.01 m between adjacent ones, as shown in Fig. 6(a). Finite element simulations are carried out to examine the effectiveness of the proposed PML prototype. Fig. 6(b) and (c) give the calculation results for two $S$-wave Gaussian beams with the angular frequency $\omega = 300\pi$ kHz, maximum amplitude $B = 100\ \mu m$ and the incident angles 90° and 45°, respectively. As can be seen from the figures, both waves are absorbed well by the proposed PML except the slight scattering in the case of oblique incidence, which is caused by the assumed square arrangement of the inclusions in this prototype. The efficiency of the PML can be further improved by dividing it into more layers and using smaller viscoelastic inclusions.

The above results show that the proposed PML can be easily fabricated and can effectively absorb elastic waves of any incident directions. At the design level, the PML is broadband provided that the quasi-static limit can be guaranteed. The

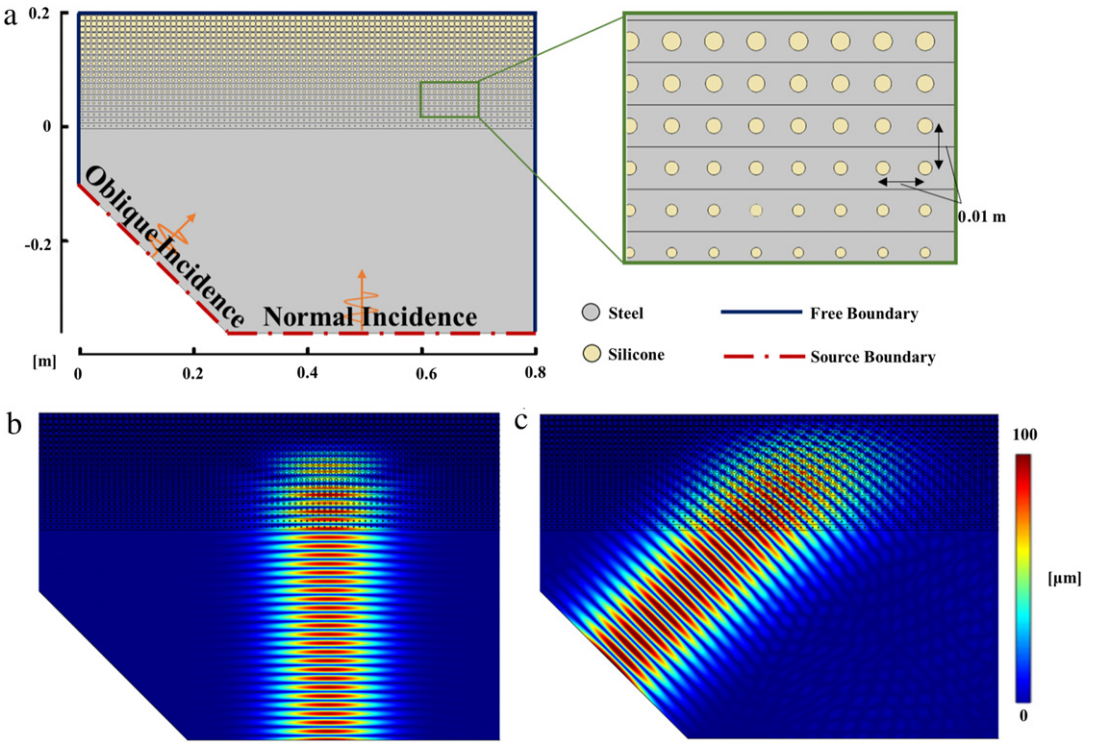


**Fig. 6.** (a) A simple PML prototype made of a viscoelastic material. (b) and (c) give the simulation results for the total wave displacement field $\sqrt{u_x^2 + u_y^2}$, where a $S$-wave with $\omega = 300\pi$ kHz impinging on the PML with incident angle 90° and 45°, respectively.

bandwidth of a PML is also limited by the selection of the viscoelastic material because of their dispersive nature of damping. The relation between the bandwidth and the viscoelastic property deserves further deep research but is omitted in this paper.

It has been reported [21,22] that the conventional PMLs will suffer from intrinsic stability problems in case the background medium is anisotropic and when "the projections of the slowness vector and of the group velocity vector have opposite signs" [22]. It is worthy to note that for the realizable PML proposed in this work, the medium of both the experimental domain and PML domains are isotropic. In this sense, the proposed PML will not suffer from the above mentioned stability problems, and long-time reliability of the proposed PML can thus be expected.

Finally, it is pointed out that the basic idea for the design of elastodynamic PMLs in this study may also be applied for some other problems where the TM holds. Take flexural (out-of-plane) waves in a thin plate as an example. In the case, the governing equation reads [23]

$$\rho^{-1/2}\nabla\cdot\{E^{1/2}\nabla[\rho^{-1/2}\nabla\cdot(E^{1/2}\nabla u_z)]\} = \beta_0^4 u_z, \tag{21}$$

where $\beta_0 = \omega^2\rho_0 h/D_0$, $D_0$, $\rho_0$ and $h$ are the flexural rigidity, normalized mass density and thickness of the plate, respectively. Eq. (21) has the property of form invariance under space transformation [23], and thus the TM can be applied. One can design realizable PMLs for out-of-plane waves in thin plates by using the above method for in-plane elastic waves.

## 4. Conclusion

Based on transformation elastodynamics, a new method has been proposed to design practically realizable elastodynamic PMLs. By applying conformal transformation technique, the elastodynamic PML is demonstrated to be realizable by using functionally graded viscoelastic materials. A prototype of such realizable PML is proposed and verified by numerical simulations. In next step, further effort will be directed to experimental validation of the proposed elastodynamic PML and its engineering applications. In addition, it will be of great interest to design more functional devices for wave manipulation or energy harvesting by integrating TM and energy conversion technique.

## Acknowledgments

The authors appreciate the efforts from Prof. Xiaoning Liu and Prof. Xiaoming Zhou and the constructive comments from the anonymous reviewers. Support from National Natural Science Foundation of China (11290153, 11221202 and 11290153) and China Postdoctoral Science Foundation (2014M550054) are acknowledged.

## References


[1] J.P. Berenger, A perfectly matched layer for the absorption of electromagnetic-waves, J. Comput. Phys. 114 (1994) 185–200.
[2] Z.S. Sacks, D.M. Kingsland, R. Lee, J.F. Lee, A perfectly matched anisotropic absorber for use as an absorbing boundary condition, IEEE Trans. Antennas and Propagation 43 (1995) 1460–1463.
[3] F.L. Teixeira, On aspects of the physical realizability of perfectly matched absorbers for electromagnetic waves, Radio Sci. 38 (2003) 8014.
[4] J.B. Pendry, D. Schurig, D.R. Smith, Controlling electromagnetic fields, Science 312 (2006) 1780–1782.
[5] U. Leonhardt, Optical conformal mapping, Science 312 (2006) 1777–1780.
[6] D. Schurig, J.J. Mock, B.J. Justice, S.A. Cummer, J.B. Pendry, A.F. Starr, D.R. Smith, Metamaterial electromagnetic cloak at microwave frequencies, Science 314 (2006) 977–980.
[7] F.L. Teixeira, W.C. Chew, Perfectly matched layers and transformation optics, in: 2009 IEEE International Symposium Antennas and Propagation, APSURSI, 1–6, 2009, pp. 3015–3018.
[8] Y. Zheng, X. Huang, Anisotropic perfectly matched layers for elastic waves in cartesian and curvilinear coordinates, in: Earth Resources Laboratory 2002 Industry Consortium Meeting, Unpublished, 2002, pp. 1–18.
[9] M. Brun, S. Guenneau, A.B. Movchan, Achieving control of in-plane elastic waves, Appl. Phys. Lett. 94 (2009) 061903.
[10] Z. Chang, J. Hu, G.-K. Hu, Transformation method and wave control, Acta Mech. Sin. 26 (2010) 889–898.
[11] J. Hu, Z. Chang, G. Hu, Approximate method for controlling solid elastic waves by transformation media, Phys. Rev. B 84 (2011) 201101(R).
[12] B.-I. Popa, S.A. Cummer, Complex coordinates in transformation optics, Phys. Rev. A 84 (2011) 063837.
[13] G.W. Milton, M. Briane, J.R. Willis, On cloaking for elasticity and physical equations with a transformation invariant form, New J. Phys. 8 (2006) 248.
[14] A.N. Norris, A.L. Shuvalov, Elastic cloaking theory, Wave Motion 48 (2011) 525–538.
[15] Z. Chang, X.N. Liu, G.K. Hu, J. Hu, Transformation ray method: controlling high frequency elastic waves (L), J. Acoust. Soc. Am. 132 (2012) 2942–2945.
[16] Z. Chang, J. Hu, G. Hu, R. Tao, Y. Wang, Controlling elastic waves with isotropic materials, Appl. Phys. Lett. 98 (2011) 121904.
[17] Y. Liu, W. Liu, X. Su, Precise method to control elastic waves by conformal mapping, Theor. Appl. Mech. Lett. 3 (2013) 021012.
[18] J. Hu, X.M. Zhou, G.K. Hu, Design method for electromagnetic cloak with arbitrary shapes based on Laplace's equation, Opt. Express 17 (2009) 1308–1320.
[19] J. Hu, X. Zhou, G. Hu, Nonsingular two dimensional cloak of arbitrary shape, Appl. Phys. Lett. 95 (2009) 011107.
[20] Detailed material parameters can be found in Cambridge Engineering Selector.
[21] E. Becache, S. Fauqueux, P. Joly, Stability of perfectly matched layers, group velocities and anisotropic waves, J. Comput. Phys. 188 (2003) 399–433.
[22] D. Komatitsch, R. Martin, An unsplit convolutional perfectly matched layer improved at grazing incidence for the seismic wave equation, Geophysics 72 (2007) 155–167.
[23] M. Farhat, S. Guenneau, S. Enoch, A.B. Movchan, Cloaking bending waves propagating in thin elastic plates, Phys. Rev. B 79 (2009) 033102.